

**THÈSE DE DOCTORAT
DE L'INSTITUT NATIONAL DES SCIENCES
APPLIQUÉES DE RENNES**

**Spécialité :
ÉLECTRONIQUE**

**Pour obtenir le grade de :
DOCTEUR DE L'INSA DE RENNES**

**Présentée par :
Anthony BOURGES**

**Faisabilité d'un radar à ondes de surface sur bouées -
Problématique de la déformation du réseau d'antennes et
réalisation d'une bouée**

Devant le jury composé de :

Rapporteurs :

Pr. Jean-Yves DAUVIGNAC

Université de Nice Sophia Antipolis

Pr. Marc HELIER

Université Pierre et Marie Curie

Examineurs :

Pr. Pierre FLAMENT

Université de Hawaii

Dr. Randy HAUPT

Pennsylvania State University

Pr. Raphael GILLARD, co-encadrant

INSA de Rennes

Dr. Régis GUINVARC'H, co-encadrant

SONDRA/Supelec

Pr. Bernard UGUEN, Directeur de thèse

Université de Rennes 1

Contents

Contents	0
1 Realization and measurement of a sea floating antenna	3
1.1 Introduction	3
1.2 Simulation of the spreading of the Bragg lines with a floating antenna	3
1.3 Introduction to the experimentations	5
1.4 WERA description	6
1.4.1 Geometry of a WERA radar	6
1.4.2 Shelter	8
1.4.3 Signal Processing of WERA	8
1.5 Building the floating antenna	9
1.5.1 Choice of the antenna	9
1.5.2 The floating antenna	10
1.5.3 The cable	11
1.5.4 The GPS	11
1.6 First measurements results	12
1.6.1 Positions of the floating antenna	12
1.6.2 Radar measurements by the floating antenna	15
1.7 Conclusion of Chapter 5	19
Bibliography	21

Chapter 1

Realization and measurement of a sea floating antenna

1.1 Introduction

In the previous chapters, we have seen that the movements of the buoys of the HFSWR alter the radiation pattern, resulting mainly in the increase of the SLL. We have proposed a correction method to attenuate these disturbances.

A second issue introduced by these movements relates to the modulation of the received signal on the moving antennas. In fact, the displacement of every elementary buoy on the sea surface, independently of the array deformation, generates some modulations in the received signal, introducing a spreading of the Bragg lines. As we have seen in Chapter 1, these Bragg lines permit to determine some oceanographic parameters, such as the wind speed or the radial velocity of the surface currents. If the positions of the Bragg Lines cannot be determine with a good accuracy, it will be useless to put the antennas on buoys for oceanographic applications. In the same way, considering the monitoring of a sea area, targets are often detected by their Doppler shift. But targets can only be detected if their radial speed is different from the Doppler frequencies of the first order Bragg lines. If the Bragg lines are spread, it means that less targets could be detected.

Some theoretical studies have been carried out on this topic. Based on [4], the signal received by one buoy has been modelled in section 1.2 to give a first insight. An experimentation is then presented, with one buoy at sea. It has been conducted using an existing oceanographic radar, replacing one of the receiving antenna by a buoy.

1.2 Simulation of the spreading of the Bragg lines with a floating antenna

This section is directly inspired from [4] which presents the perspective to use a receiving array of antennas on barges. This article presents suitable results with a limited

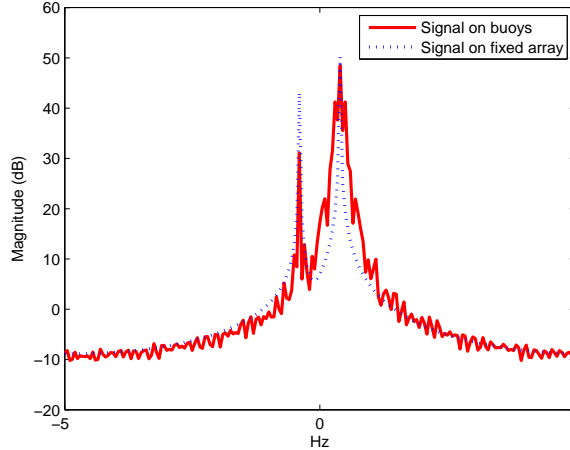


Figure 1.1: Comparison of a Doppler cut between a fixed antenna and a floating antenna.

spreading of the Bragg lines for a sea state 3.

The signal received on the floating antenna is studied taking into account the roll, the pitch and the displacement of all the antennas of the receiving array. The different degrees of freedom are defined using the modelling of the buoy movement presented in Chapter 2. The simulation was computed with a global acquisition time of 20 s, considering a pulsed radar transmitting at 15 MHz. Then, a range Doppler representation of the received signal is computed to quantify the disturbances.

Fig. 1.1 presents a cut of the range Doppler map. It compares the Bragg lines of one fixed antenna and the Bragg lines of one floating antenna. We can clearly see for the floating antenna a spreading of the positive Bragg line and a strong attenuation of the negative Bragg line. Both effects would totally alter the calculations of the corresponding oceanographic parameters. In addition, the spreading of the positive Bragg line would possibly hide some targets for the monitoring applications.

However, contrary to the modelling of the array in the previous chapters, the time evolution of the tilt angle is here the most important point defined in [4]. Obviously, it cannot be described with a fine accuracy in our model. As a consequence, we can only conclude that the disturbances generated by the roll, the pitch and the buoys displacements can strongly modify the Doppler representation and that a real measurement is needed.

The next parts of this chapter are thus focused on the experimentations we have realized with a floating antenna. They permit to quantify the disturbances generated by the movement of the sea and more particularly the spreading of the Bragg lines in real conditions.

1.3 Introduction to the experimentations

Next to the city of Porspoder in French Brittany (cf. Fig. 1.2), on the 'La Garchine' cape, the French navy hydrographic and oceanographic department (SHOM), in collaboration with the company Actimar, is operating an experimental HFSWR to measure the current in the Iroise sea. It has been in use for two years and will continue for at least two other years. It is therefore a reliable radar, allowing us to focus on the floating antenna conception. Furthermore, this experiment was conducted in collaboration with Prof Pierre Flament, from the University of Hawaii, who already knows the functioning of this particular radar. Finally, the logistic was quite easy there, there are many ports with all the necessary marine shops. The radar is a WERA system, built by Helzel



Figure 1.2: Localization of Porspoder in French Brittany

messtechnik (Hamburg, Germany). It is a phased array system, in a quasi-monostatic configuration. The basic idea of this experiment was to replace one of the receiving antenna by a floating antenna (cf. Fig. 1.3). The term 'floating antenna' refers to the platform with the antenna and the other equipments. An additional long coaxial cable is used to link the floating antenna to the position of the fixed turned off antenna. This way, all the radar infrastructure can be reused.

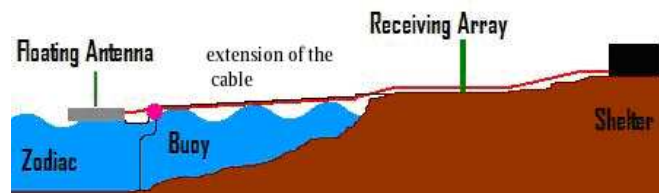


Figure 1.3: Presentation of the experimentation

1.4 WERA description

In the oceanographic domain, two oceanographic HFSWR are usually used: the first is the Coastal Ocean Dynamics Applications Radar (CODAR) developed by Barrick [2]. The second one is the WERA system (Wellen Radar) which is a shore based remote sensing phased array system, originally developed at the university of Hamburg by Klaus-Werner Gurgel et al. [3]. Both can be used to measure the ocean surface currents and the wind speed and direction. SHOM has chosen to operate a WERA.

1.4.1 Geometry of a WERA radar



Figure 1.4: Air picture of the Porspoder site

The geometry is illustrated in Fig. 1.4. The transmitting and receiving array are positioned along the coast. The radar operates in a frequency modulated continuous wave mode (FM-CW), it thus emits continuously a very low power, without any gating nor pulsing sequence. As a consequence, the receiver has to be located in a null of the transmitter to suppress the direct signal from the emitter.

A transmitting array of 4 antennas (cf. Fig. 1.5) is thus used. The shape of the array and the phases applied to the antennas permit to form a main beam toward the sea with a zero in the orthogonal direction where the receiving array is located. Its array factor is plotted in Fig. 1.6.



Figure 1.5: Transmitting array of a WERA radar.

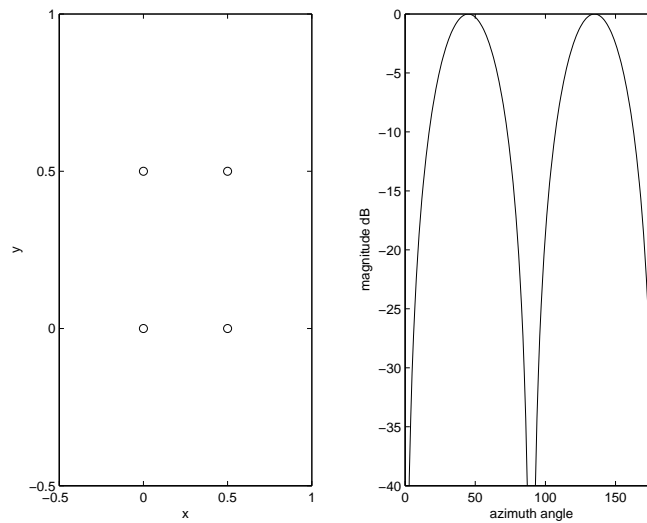


Figure 1.6: Antennas positions in wavelength of the transmitting array with its associated array factor.

The receiving array is a regular linear array of 16 antennas with a half wavelength spacing. The receiver is continuously switched on. The signals from 16 antennas are processed in parallel. It has a typical azimuthal resolution of 3° .

By convention, antenna 1 is the nearest to the emitter, antenna 16 is the furthest.

The location of the floating antenna should be carefully chosen. This floating antenna will be linked by a cable to the fixed antenna it will replace. This cable should be as short as possible. Two locations are therefore possible, marked by a red dot and a white dot in Fig. 1.4. In addition, in order to suppress the direct signal, it must be located in the null of the transmit array. Only the red dot fullfills this last condition.

Consequently, the fixed antenna which will be disconnected is antenna 16 (to shorten the additional cable).

1.4.2 Shelter

The shelter houses all the electronics of the WERA (cf. Fig. 1.7), the receiving part as well as the transmitting part.

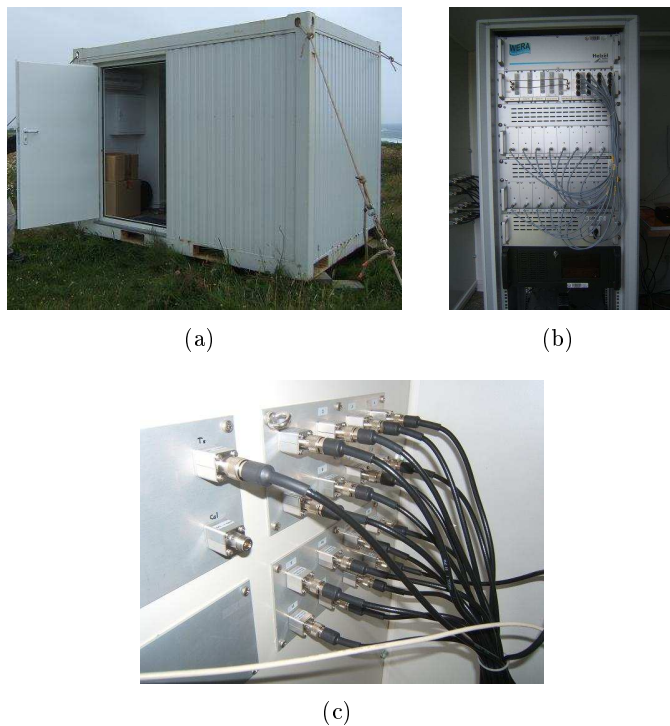


Figure 1.7: Picture of the Shelter (a), acquisition system of the WERA (b) and the input of the transmitters and the outputs of the 16 receiving channels (c) which are inside the shelter

All separated received signal from the 16 antennas are digitally registered. So the signals of each antenna can be observed, independently of the others. In particular, the signal coming from the buoy will be extracted.

1.4.3 Signal Processing of WERA

The signal processing in WERA consists in a range Doppler analysis of the back scattered signals for each channel (or antenna) of the receiving array.

The range Doppler processing is illustrated in Fig. 1.8 and was explained in the first chapter. The transmitting signal is a frequency ramp. The time length for one chirp is T_r and there are N_{chirp} chirps. So, the total integration time is $T_r N_{chirp}$. The

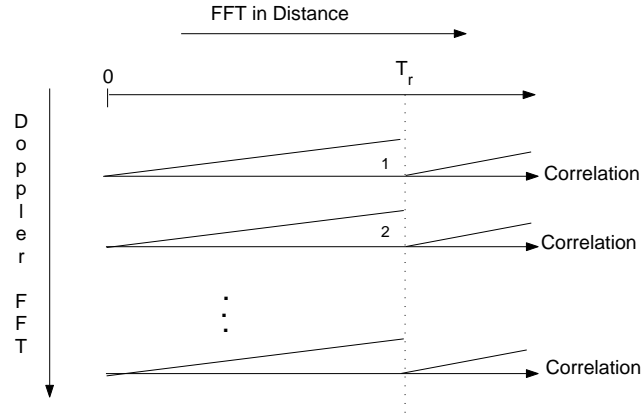


Figure 1.8: Range Doppler processing with a WERA

maximum Doppler frequency f_{max} is then:

$$f_{max} = \frac{1}{2T_r} \quad (1.1)$$

with a Doppler resolution Δf of:

$$\Delta f = \frac{1}{T_r N_{chirp}} \quad (1.2)$$

The range resolution is $\frac{c}{2B}$, with B the bandwidth of the chirp and c the celerity (cf. Chapter 1). Normally, a 100 kHz bandwidth is chosen, corresponding to a range resolution of 1.5 km. A typical work frequency is equal to 12.5 MHz. In order to observe the slow ocean parameters, the received signal is typically integrated over 10 min.

1.5 Building the floating antenna

1.5.1 Choice of the antenna

The disconnected antenna of the receiving array can not be used for the experimentation as it is too large. An active antenna is chosen instead. It is made by Rhode and Shwartz (cf. Fig. 1.9) and it is referenced “HE011 Aktivantenne” [1]. Its output power is the same as the passive antennas used in the WERA.



Figure 1.9: HE011 Rohde & Schwarz Aktivantenne

1.5.2 The floating antenna

The floating antenna is composed of two main elements, a hermetic box and a small boat.



(a)



(b)

Figure 1.10: (a) the hermetic box and (b) the zodiac.

The hermetic box permits to protect all the electronics boarded on the floating antenna from the projections of sea water. Inside, we distinguish a GPS RTK and an inertial central (presented in the next section). The active antenna is attached outside the box (cf. Fig. 1.10(a)).

The zodiac is the platform which permits the hermetic box to float. The zodiac is not directly anchored to the seabed. A buoy is used to limit the mechanical tensions generated by the sea movement. It has to be noted that using this kind of boat as a

measurement platform is not optimum because it is floating on top of the waves. Thus, it is subject to all the sea movements, even the high frequency ones.

1.5.3 The cable

A 300 m coaxial cable is used to link the floating antenna to antenna 16 in the receiving array. The first part of the cable is on the ground, between the free connector of antenna 16 and the edge of the rocks along the coast. The second part is between the rocks and the floating antenna. This last part will move with the sea elevation and the tide and it must therefore be protected. To this end, a floating electrical sheath is added. Each of the ends of the electrical sheath is filled with polyurethane foam, to prevent the sea water from entering into the sheath.



Figure 1.11: The cable with its yellow sheath (a) when the sea is high (b) when the sea is low with a lot of rocks

A picture of the cable with its protection is in Fig. 1.11. We can see that the floating cable follows the sea elevation, limiting the frictions on the rocks generated by the sea movement.

1.5.4 The GPS

A GPS in RTK mode is used to know with accuracy the successive positions of the floating antenna. It is composed of two parts. The first one, called base, is fixed and is used as a reference and the second one, called mobile, is on the floating antenna. A UHF link between the base and the mobile permits to improve the accuracy of a normal GPS down to centimeter. Each part is composed of:

- a GPS antenna to receive the signals from the satellites,
- an independent battery which guarantee an autonomy of 10 hours at sea,



Figure 1.12: (a) Picture of the GPS base near antenna 16 (b) Picture of the GPS module in the hermetic box of the floating antenna.

- an acquisition card,
- a VHF module for the communication between the mobile and the base.

An inertial central is used to measure the roll and the pitch of the floating antenna during the experimentation.

The next section presents the results of the first measurements

1.6 First measurements results

We will first have a look at the movements of the floating antenna in order to evaluate their magnitude.

1.6.1 Positions of the floating antenna

Fig. 1.13 shows the latitude and the longitude in degree of the floating antenna measured by the GPS RTK during all the experimentation, from the departure at the nearest beach (top right of the figure) to the return to the same beach. Fig. 1.14 is a zoom of the bottom left part of Fig. 1.13, representing the positions of the floating antenna when it is anchored during the radar acquisitions. The coordinates have been transformed to meter. The ways in (to deploy the floating antenna) and out (to bring back the floating antenna to the beach) are indicated. It clearly shows that the floating antenna has evolved in a 10m*10m square during the 4 hours of measurements.

Fig. 1.15 represents the altitude of the floating antenna. The reference time $t=0h$ is when the GPS has been turned on on the beach before closing the hermetic box. Then, 3 hours were necessary to anchor the floating antenna and to deploy the floating cable

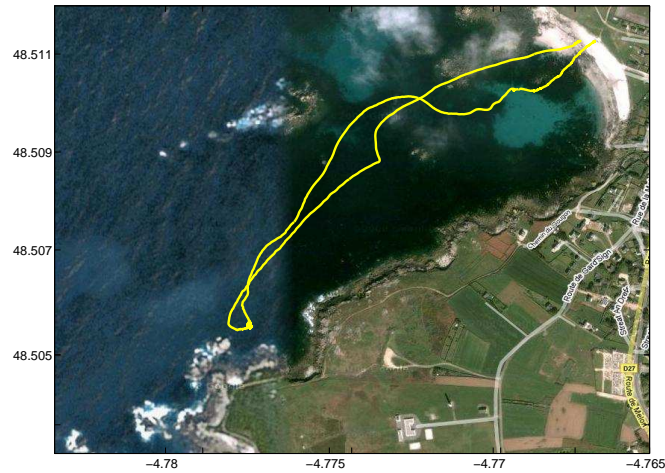


Figure 1.13: Latitude and longitude of the floating antenna during all the acquisition.

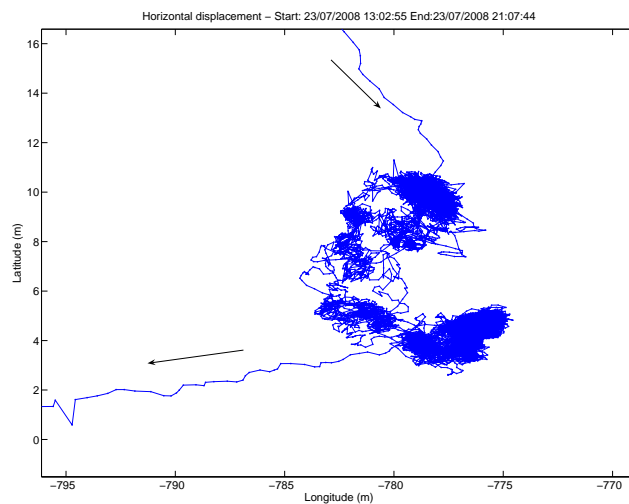


Figure 1.14: Positions of the floating antenna around its anchorage during the measurements.

for the measurement of the signal of the floating antenna. When the floating antenna was alone (after $t=3h$), it was no longer disturbed by a human activity, the curve becomes smooth. At the same time, we have started to record the signal. The continuous increase of the altitude of the floating antenna corresponds to the tide effect which has increased the sea elevation during the experimentation time. At the end of the recording

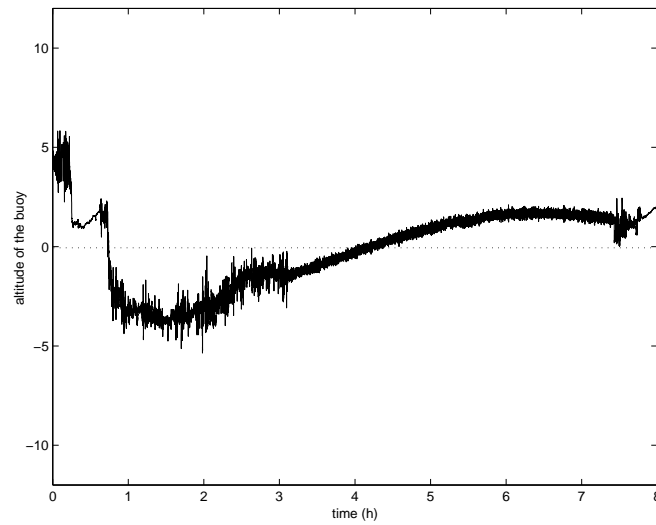


Figure 1.15: Altitude of the floating antenna in meter during all the acquisition.

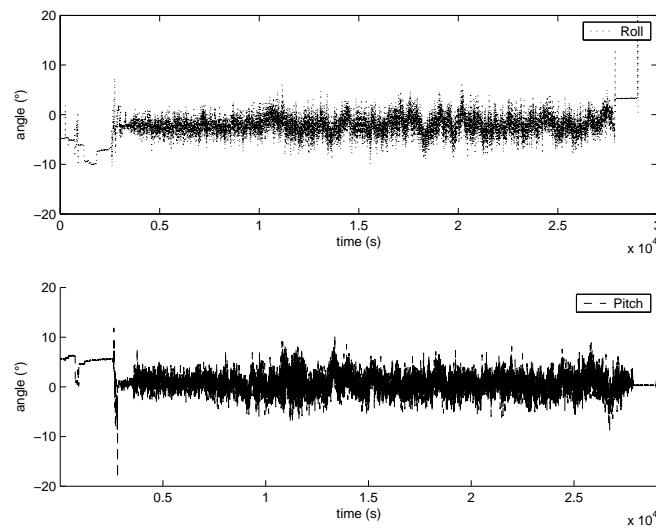


Figure 1.16: Pitch and Roll of the floating antenna

($t=7h$), the curve of the altitude is no longer smooth because of the human activity to bring it back to the beach. The vertical motion during each measurement movements appears to have been very low, less than 1 meter.

In the same way, the pitch and roll were measured. Their curves are represented in Fig. 1.16. Their movements appears to be very weak, $\pm 5^\circ$. This point is highly interesting for our problem as it implies that the modulation of the received signal should

not be too strong. We can also notice that the pitch is centered around zero while the roll has a small shift, around 2° .

1.6.2 Radar measurements by the floating antenna

A first run was done with the standard parameters of the radar: 4096 chirps of 0.26s. Using Eq. 1.1 and Eq. 1.2, this corresponds to a maximum Doppler frequency f_{max} of 1.92 Hz and a Doppler resolution Δf of $9.40 \cdot 10^{-4} Hz$. The central transmitting frequency was 12.48 MHz (automatically chosen by looking for a free part of the spectrum) with a bandwidth equal to 100 kHz. The 16 signals were processed as previously described. The range Doppler representation of the floating antenna is plotted in Fig. 1.18. The result of antenna 15 is also provided as a reference.

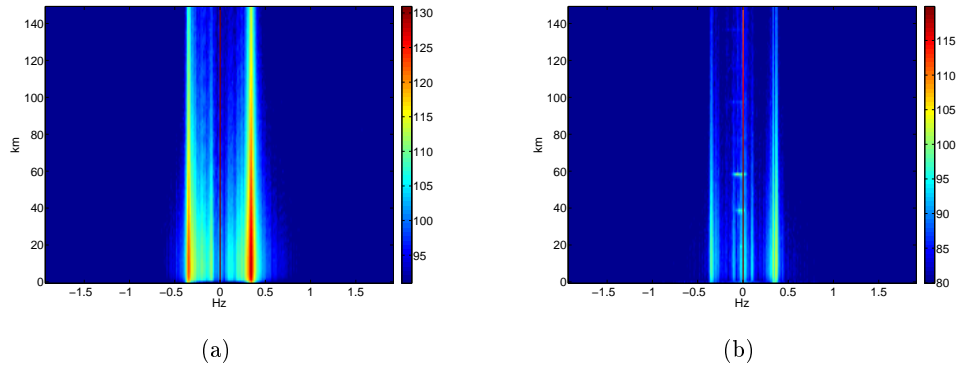


Figure 1.17: Range Doppler representation (a) of antenna 15 and (b) of the floating antenna.

A first look at the results shows that the signal of the floating antenna has a lower magnitude. As expected, we can see the first order Bragg lines and a zero Doppler component. Fig. 1.18 shows a cut at 70 km of these two results, along with the result of antenna 1. The difference in magnitude between antenna 15 and antenna 1 is also large. The signal (defined as the maximum of the negative Bragg line) to clutter (defined as the signal outside the Bragg lines) ratios of antenna 1 and of antenna 15 are roughly 25 dB while for the floating antenna it is only 15 dB. A 8-dB attenuation of the clutter between antenna 15 and antenna 1 is represented. The shelter is actually located near antenna 1, so there is some additional cable to link antenna 15 to the shelter. This explains the difference in magnitude between antenna 1 and antenna 15.

Considering the floating antenna, there is a 14-dB difference of the magnitude of the clutter with antenna 15 and a 22-dB difference of the level of the Bragg lines. Once again, the cable explains some of the difference: a 300 meters cable is used to link the position of antenna 16 to the floating antenna. This cable has an attenuation of about 12 dB (1.2 dB for 100 feet in a cable RG 213 at 30 MHz). There is also a few additional meters of cable between antenna 15 and antenna 16. But this does not explain the

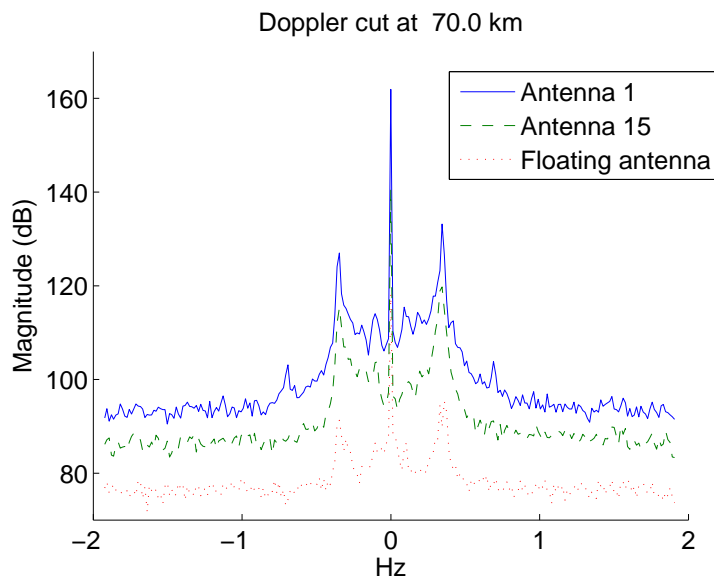


Figure 1.18: Doppler plot at 70km for antenna 1, antenna 15 and the floating antenna.

loss of signal to clutter ratio. The connections of the floating cable were not properly soldered and the edge connected to the floating antenna has been oxydized. Another possible reason we hadn't time to check is that the signal of the floating antenna might be too low for the radar, in other words the signal outside the Bragg lines is not the clutter but the radar noise.

So regarding the magnitude of the signal, the floating antenna shows some losses. But it seems to be able to correctly detect the Bragg lines. We have then normalized the signal of antenna 15 and of the floating antenna to the same reference for a thorough study of these Bragg lines. This is plotted in Fig. 1.19.

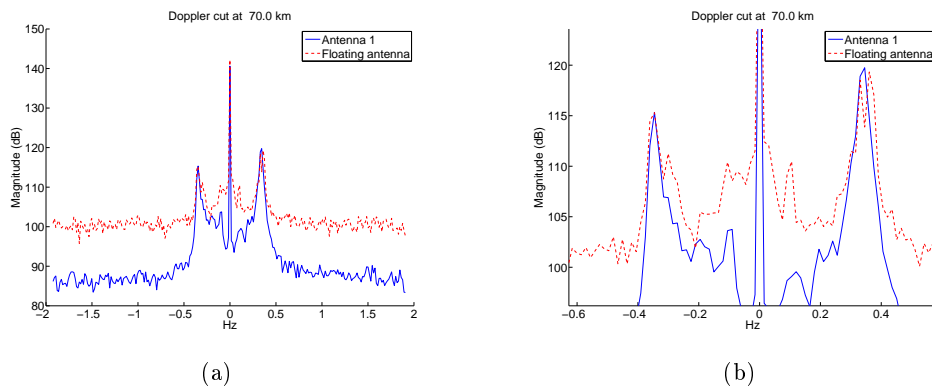


Figure 1.19: (a) Normalized Doppler cut at 70 km, and (b) zoom on the first order Bragg lines.

A small spreading of these Bragg lines is visible (particularly on the negative line) but it is very limited. The positive line seems to be slightly splitted. But globally, the Bragg lines are found in both cases at $f_b = \pm 0.36$ Hz, corresponding to a frequency equals to 12.34 MHz, with roughly the same maximum. So, it appears that the floating antenna can find the correct location of the Bragg lines, along with the correct ratio of these two lines. It is therefore suitable for oceanographic applications. These Bragg lines are not broaden too much by the sea surface movements, so the floating antenna can also be used for monitoring applications. However, for the latter application, an indepth study has to be carried out on the signal to clutter ratio.

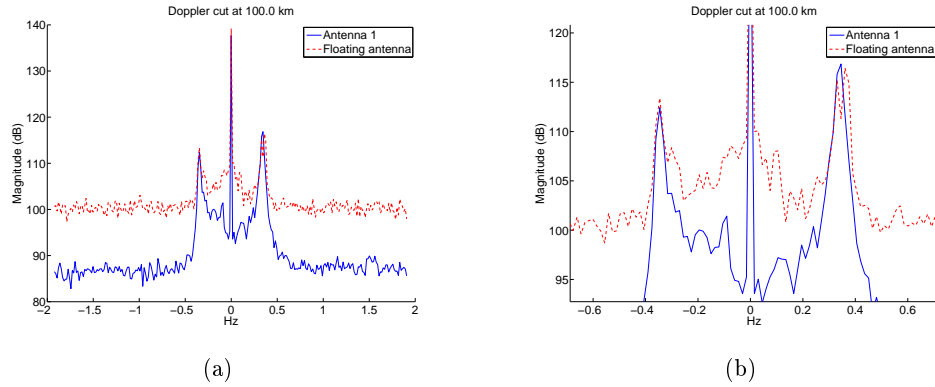


Figure 1.20: (a) Normalized Doppler cut at 100 km, and (b) zoom on the first order Bragg lines.

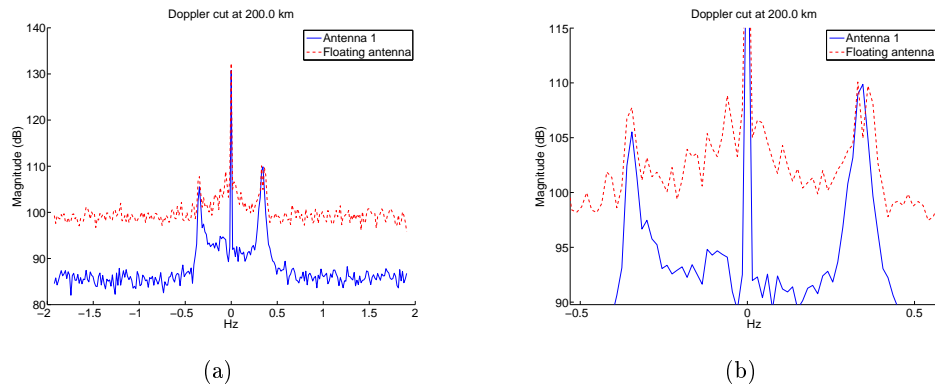


Figure 1.21: (a) Normalized Doppler cut at 200 km, and (b) zoom on the first order Bragg lines.

Fig. 1.20 and Fig. 1.21 show two other cuts, at 100 km and 200 km respectively. The conclusions of the cut at 70 km also apply. It is interesting to note that the floating antenna performs still well at 200 km: although the signal to clutter ratio is only 5 dB, the Bragg lines can still be clearly identified.

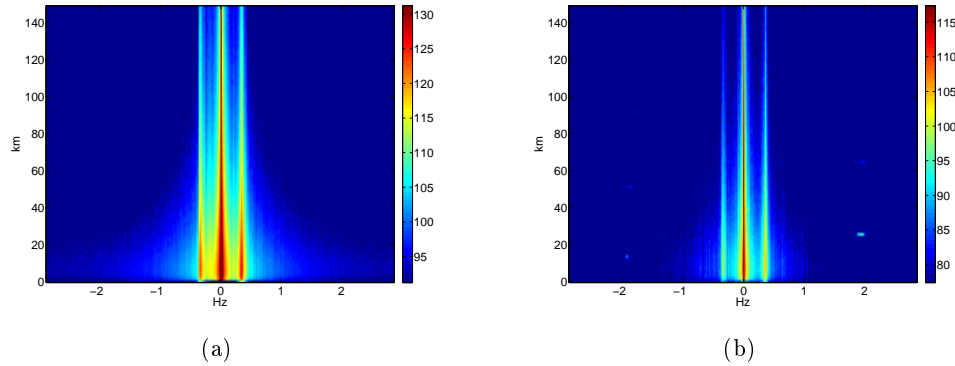


Figure 1.22: For run 2, Range Doppler representation (a) of antenna 15 and (b) of the floating antenna.

Several other runs were realized, with the same conclusions. In particular, the chirp length has been varied. In Fig. 1.22, the chirp length is 0.1733s. Following Eq. 1.1 and Eq. 1.2, the decrease of T_r permits to see higher Doppler frequencies $f_{max} = 2.89Hz$, but with a lower Doppler resolution $\Delta f = 1.41 \cdot 10^{-3} Hz$. The Bragg lines are found at the same position.

This first measurement has validated the feasibility of the floating antenna. Measurements with stronger sea states are however needed. It will also be interesting to do them with improved platforms, such as the one on Fig. 1.23. The latter, realized during the Porspoder experimentation, is designed to cut the high frequency waves. But a heavy sea state has prevented us from putting it at sea.

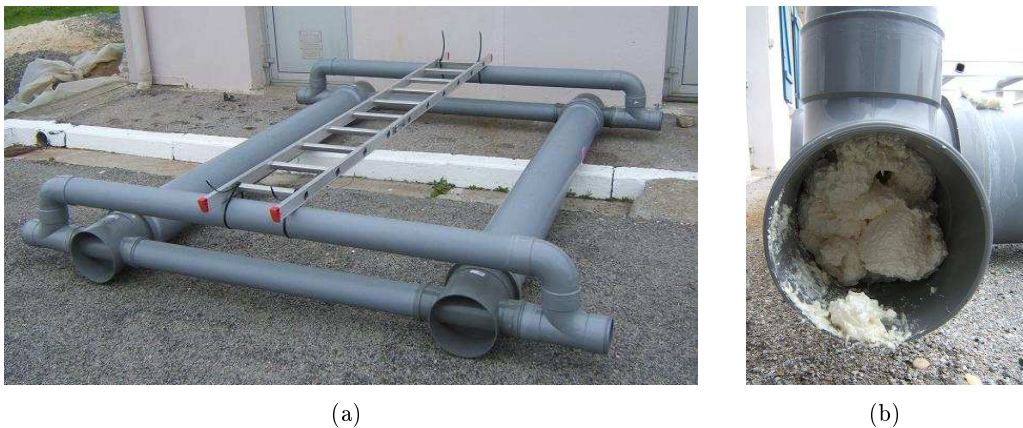


Figure 1.23: Floating platform and a tube of the platform which filled with polyurethane foam

1.7 Conclusion of Chapter 5

These experimentations have validated the feasibility of a sea floating antenna. A simple and cheap sea floating antenna has been realized and measured, with a calm sea. The measurements have shown that the sea floating antenna was able to correctly measure the Bragg lines and that it was thus suitable for oceanographic applications. It has also shown that the Bragg lines are only very slightly spread by the sea surface movements. The monitoring application can therefore be also envisaged. However, the signal to clutter ratio issue has to be further investigated. Other measurements with improved platforms and different sea states must be done. These future measurements have also to include the complete array of floating antennas.

Bibliography

- [1] <http://www.ratzer.at/pdf/he011.pdf>, 2007.
- [2] D. Barrick, M.W. Evans, and B.L. Weber. Ocean surface current mapped by radar. *Science* 198, 1977.
- [3] K.-W. Gurgel, G. Antonischti, H.-H. Essen, and T. Schlick. Wellen radar (wera): a new ground-wave hf radar for ocean remote sensing. In *Coastal Engineering*, 2000.
- [4] J. Wang, R. Dizaji, and A.M Ponsford. An analysis of phase array radar system on a moving platform. In *IEEE*, 2005.